LCLS-TN-23-1
January 8, 2023

HXRSS Chicane Modification

Heinz-Dieter Nuhn[a]

[a]SLAC National Accelerator Laboratory, Stanford University, CA 94309-0210, USA

ABSTRACT

The LCLS-II-HE project at SLAC is proposing an upgrade of the HXRSS crystal chamber, currently installed on the movable girder in LCLS-II HXR cell 28 in the center of a 4-dipole-chicane. The proposed upgrade will provide cryo-cooling for the diamond crystal to make it capable to cope with the upcoming high pulse repetition rate. The cryo-cooling upgrade requires an increase of the outside dimensions of the crystal chamber. To accommodate the larger chamber, the project proposes relocating the two center dipoles of the chicane away from the chicane center by 0.101681 m, each. This technical note discusses the consequences of such a relocation.

Keywords: Chicane

1. INTRODUCTION

SLAC has implemented hard x-ray self-seeding (HXRSS) in its LCLS FEL in 2011. The main components include a 4-dipole chicane and a diamond crystal chamber mounted on one of the movable girders that normally each carry an undulator segment. The system was successfully commissioned in January 2012 as part of the original LCLS undulator line. During the 2019/2020 upgrade of the LCLS undulator line with the then new LCLS-II HXR undulator line components, the HXRSS chicane girder components were transferred from the old LCLS-style steel girder to a new LCLS-II-style aluminum girder but were otherwise kept unchanged. The system was commissioned again with the beam from the Cu linac and is currently operational. Soon, commissioning of the HXR undulator line with the beam from the new superconducting (SC) linac will begin. The SC linac will eventually be able to deliver much higher beam power levels (high bunch repetition rate) than the Cu linac is able to and it is estimated and has been shown experimentally that the high bunch rate will distort the diamond crystal in its current configuration due to heating by the rapid succession of x-ray seeding pulses hitting the crystal, which, in turn, will spoil self seeding. A mitigation, proposed by the LCLS-II-HE upgrade project, currently in preparation, will cryo-cool the crystal, thus avoiding high temperature build-up. The cryo-cooling addition requires to increase the outside dimensions of the crystal chamber, which is mounted between the two central dipoles of the four-dipole chicane. In order to still fit the new crystal chamber in the center of the chicane, dipoles 2 and 3 will have to be repositioned such that the spacing between the two is increased by 0.20362 m. This will be accomplished by relocating each of these two dipole magnets by 0.101681 m away from the center. The effect, that this change will have on the chicane parameters, is described in this note.

Table 1: Dipole magnet parameters of the current HXRSS and planned HXRSS-HE chicane assemblies.

Parameter Name	Symbol	Current	Proposed	Change
Dipole Core Length	L_d	0.3556 m	0.3556 m	0.00%
Distance between centers of first two dipoles*	$\Delta L_{s,12}$	0.9568 m	0.8551 m	-10.65%
Distance between centers of middle two dipoles	$\Delta L_{s,23}$	0.9360 m	1.1394 m	+21.73%
Distance between centers of last two dipoles*	$\Delta L_{s,34}$	0.9568 m	0.8551 m	-10.65%
Total Chicane Length†	L_{total}	3.2052 m	3.2052 m	0.00%

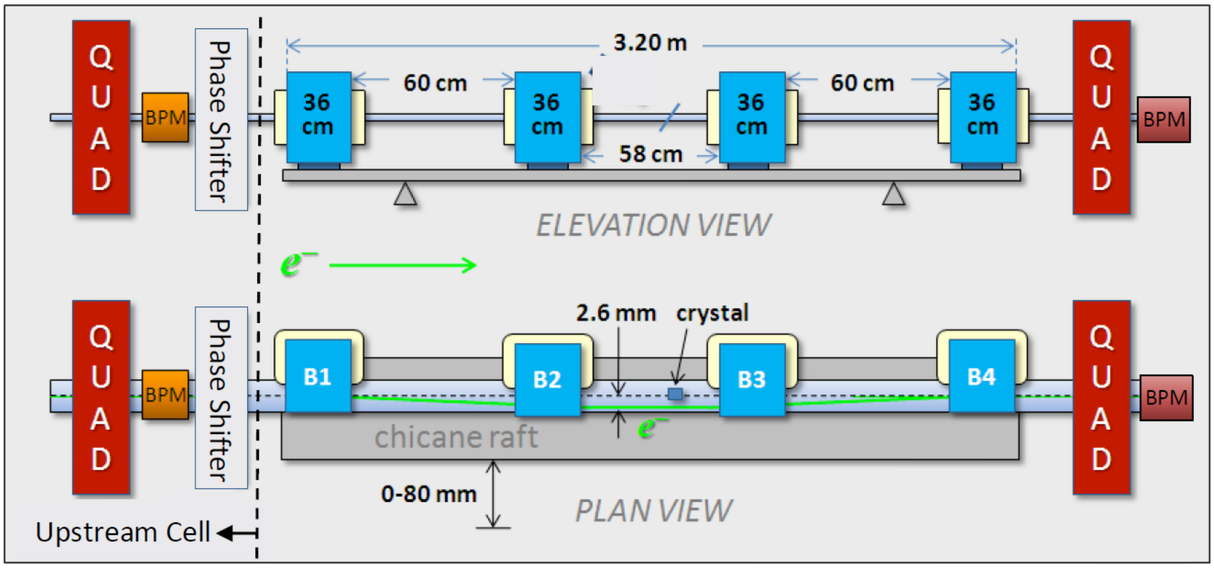

Figure 1: Schematic elevation and plan views of the HXRSS chicane in HXR cell number 28, with parameters shown ("aisle" side is above the "plan view"). Beam passes from left to right in this figure. Lengths are from steel edge to steel edge. (The figure is taken from the Physics Requirements Document (PRD) [1])

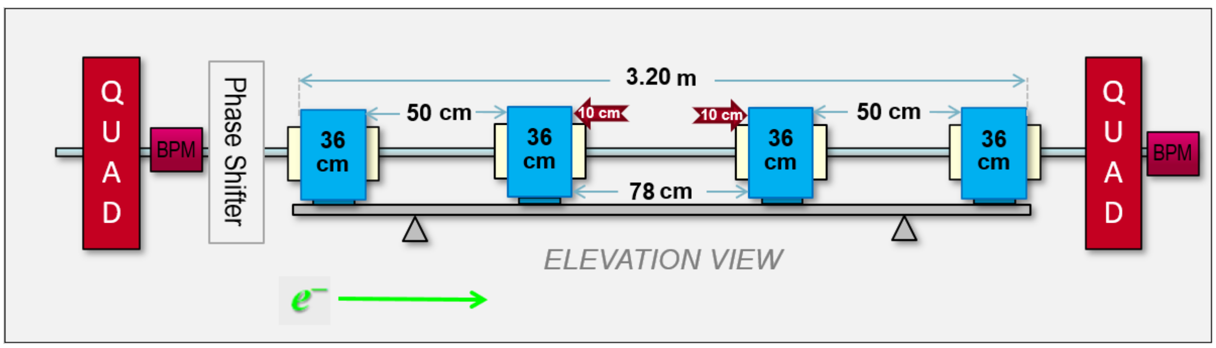

Figure 2: Schematic elevation view showing the changes proposed to the current HXRSS chicane for the HE upgrade, indicated by the two horizontal red arrows, labeled "10 cm".

2. CHICANE DESCRIPTION

Figure 1, a diagram taken from the HXRSS physics requirements document [1], shows the longitudinal positions of the dipole magnets of the four-dipole chicane currently mounted on the HXRSS girder in cell 28 of the LCLS-II HXR undulator beamline. While the current document was being prepared, it was found that the dipole spacings in the MAD deck differ from the ones specified in the PRD. Metrology measurements confirmed that the actual longitudinal spacings of the dipoles agree with the PRD request. The location values in the MAD deck will be corrected. The relocations of the center two dipoles as proposed by the upgrade to HXRSS-HE are depicted in Figure 2. The chicane dipole separation $\Delta L_{s,23}$ is to be increased by about 22% while separations $\Delta L_{s,12}$ and $\Delta L_{s,34}$ are to be reduced by about 11%. Precise position parameters of the chicane dipole magnets as they are now and how they are to be after the change are listed in Table 1.

3. UPGRADE IMPACT

Next, we analyze how the proposed changes in dipole positions will affect chicane parameters during operations with the electron beam. The integrated magnetic dipole field $(BL)_{dipole}$

Further author information: E-mail: nuhn@slac.stanford.edu
*Distances between magnet centers are based on metrology measurement rather than MAD coordinates.
†Distance between the start of the 1st and the end of the last dipole magnet core

$$(BL)_{dipole} = \int_0^{L_d} B_y(z)\, dz, \tag{1}$$

can be changed during beam operation between 0 Tm and 0.19 Tm. (The measured maximum integrated field amplitudes for the four chicane dipole magnets at the maximum MCOR power supply current of 6 A are {0.1926 Tm, 0.1914 Tm, 0.1928 Tm, 0.1923 Tm}. For degaussing purposes, the field integral can be changed in the, roughly, ± 0.19 Tm range, which is allowed by the MPS system if no electron beam is present). Besides being limited by the power supply capacity, the maximum and minimum integrated field integrals are also restricted by the in-vacuum geometry between the center two dipole magnets.

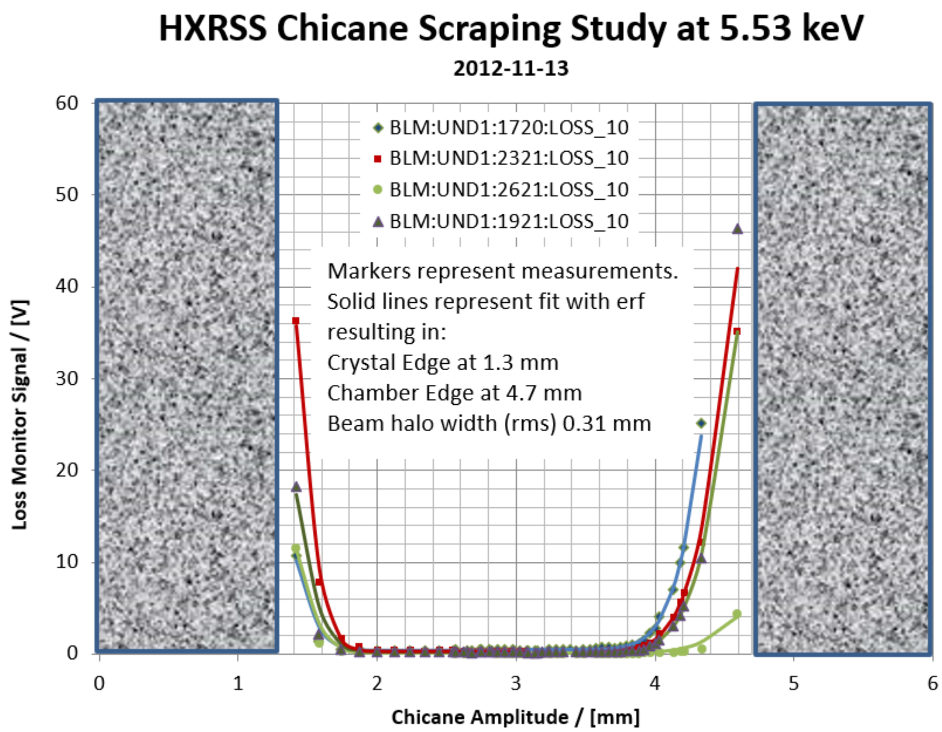

Figure 3: Result of chicane amplitude limiations measured on 11/13/2012 on the first HXRSS installation.

Figure 3 shows measurements done on the first installation of the HXRSS system, which was part of the original LCLS undulator beamline, to determine the chicane bump limitations. The horizontal axis shows the maximum deflection of the charge center of the electron bunches at the longitudinal chicane center. The bunch deflection was controlled through the integrated chicane dipole current at an electron beam energy of $E_e = 11.159$ GeV. The vertical axis shows the readings (in units of mV) of some of the beam loss monitors (BLMs) located downbeam of the chicane girder at distances of 1 girder (blue diamonds), 3 girders (blue triangles), 7 girders (red squares) and 10 girders (olive circles). As can be seen in the figure, choosing a chicane amplitude either too small or too large will generate beam loss. The loss at the smaller chicane amplitudes comes from the electron bunches getting too close to the diamond crystal edge, which was estimated, based on these measurements, to be at about 1.3 mm chicane amplitude. The loss at the larger chicane amplitudes comes from the electron bunches getting too close to the vacuum chamber or too close to bellows. The equivalent chicane amplitude that corresponds to those obstacles was estimated to be about 4.7 mm. By looking more closely at the figure, the difference between the two scattering events becomes apparent. The beam loss from scattering on the diamond crystal (left side) is most strongly detected by loss monitors that are located further downbeam from the crystal (see the red squares in the figure, i.e. the readings from a beam loss monitor located 7 girders or about 28 m downstream of the chicane). This is because the rather weak scattering on the thin diamond crystal only increases the divergence of electrons, which then have to travel a distance before they reach the vacuum chamber, where their energy gets fully converted into radiation that can be detected at the outside of the vacuum chamber. The beam loss from scattering on the vacuum chamber components (right side), on the other hand, will immediately cause the energy of the electrons to be converted to outside radiation and is detected by beam loss monitors that are much closer to the chicane (see the blue diamonds in the figure, i.e. the readings from a beam loss monitor located 1 girder or about 4 m downstream of the chicane). In order to avoid the generation of radiation, the chicane amplitude was administratively restricted to 4 mm. As mentioned in the Introduction, the transfer of chicane girder components during the transition to the LCLS-II HXR line should not have significantly changed the geometry of the chicane dipoles arrangement and the vacuum chamber. To be sure about the new bump limitation the 11/13/2012 measurement should be repeated. Until then, we will be using the same numbers. A consequence of keeping the maximum chicane amplitude at or below 4 mm is that for electron beam energies below 13.625 GeV the maximum allowed integrated magnetic field is limited to below 0.19 Tm. Of importance for the self-seeding operation is the maximum photon energy, E_{ph}, which is related to the electron energy through the undulator period length, $\lambda_u = 0.026$ m and the maximum value of the undulator parameter $K_{max} = 2.57$ by

$$E_{ph,min} = \frac{2hc\gamma^2}{\lambda_u \left(1 + K_{max}^2/2\right)}, \tag{2}$$

with the relativistic Lorentz factor, $\gamma = E_e/\left(m_e c^2/e\right)$, using the electron rest energy, $m_e c^2/e$=510998.95 eV, Planck's constant, $h = 6.62607015 \times 10^{-34}$ Js, and the speed of light in vacuum, c=299792458 m/s.

Additional parameters relevant for chicane characterization include:

- the bend angle, Θ_{bend}, of the first‡ chicane magnet

$$\Theta_{bend} = \frac{(BL)_{dipole}}{B\rho}, \tag{3}$$

  using the rigdity $B\rho = E_e/(ec)$, where e=1.60217663×10^{-19} C is the electron charge;

- the maximum horizontal displacement of the electron beam in the chicane center, $\Delta x_{chicane}$§

$$\Delta x_{chicane} = 2\rho_{dipole}\left(1 - \cos\left(\Theta_{bend}\right)\right) + \left(\Delta L_{s,12} - L_d\right)\tan\left(\Theta_{bend}\right) \approx \frac{L_d \Delta L_{s,12}}{\rho_{dipole}} \approx \Theta_{bend}\Delta L_{s,12}, \tag{4}$$

  with $\rho_{dipole} = L_d/\sin\left(\Theta_{bend}\right) \approx L_d/\Theta_{bend}$;

- the phase integral, PI

$$PI = \int_0^{L_{total}} \left(\int_0^{\bar{z}} B_y\left(\bar{\bar{z}}\right) d\bar{\bar{z}}\right)^2 d\bar{z} = (BL)_{dipole}^2 \left(\Delta L_{s,12} + \Delta L_{s,34} - \frac{2}{3}L_d\right); \tag{5}$$

- the extra path length through the chicane, Δs_c

$$\Delta s_c = \frac{PI}{2\left(B\rho\right)^2}; \tag{6}$$

- the time delay, Δt_c

$$\Delta t_c = \frac{\Delta s_c}{c\sqrt{1 - 1/\gamma^2}} \approx \frac{\Delta s_c}{c}; \tag{7}$$

- and the bunch lengthening per 100% energy spread, R_{56}

$$R_{56} = 2\Delta s_c \approx 2c\Delta t_c. \tag{8}$$

.

‡Note: The bend angles of the four chicane dipoles are Θ_{bend}×{1.000,-0.994,-1.001,0.999}.

§Note: For this and the following parameters it is assumed that the trim windings on the 3 downbeam chicane dipoles are used to equalize the absolute values of the 4 bend angles to close the bump in the electron beam trajectory due to the chicane fields. Without this, the bump would not be closed and would cause a betatron oscillation downstream of the chicane, which is undesirable.

The proposed change in chicane dipole separations $\Delta L_{s,12}$ and $\Delta L_{s,34}$ will affect chicane performance, while the change in separation $\Delta L_{s,23}$ will not. If beam energy and dipole fields are kept constant, $\Delta x_{chicane}$ will change linearly with the chicane separation (i.e., by -10.6%) while parameters PI, Δs_c, Δt_c and R_{56} will change a bit more (-12.1%). The change of those chicane parameters can be mitigated by increasing the dipole field by 7.5%. With that adjustment, Θ_{bend} will increase by the same amount but $\Delta x_{chicane}$ will decrease by 4.0% and parameters PI, Δs_c, Δt_c and R_{56} will remain unchanged. This mitigation can be applied up to an electron energy of 12.75 GeV (13.8 keV). At that energy, the correction increases the integrated dipole field to its limit value of 0.19 Tm. This is not the highest energy at which the modified chicane can be operated. That energy is 13.625 GeV (15.759 keV), at which the integrated chicane dipole field for the current positions is at the maximum value of 0.19 Tm. Since in this case the mitigation can no longer be applied after the proposed upgrade, the Time Delay must be reduced from 48.9 fs to 42.9 fs. Numerical values for these two cases are listed in Table 2.

Table 2: Parameter comparison between the current HXRSS chicane and the proposed HXRSS-HE chicane for the two limiting cases described in the text.

Parameter Name	Symbol	Current HXRSS		Proposed HXRSS-HE		Units
Electron Energy	E_e	12.750	13.625	12.750	13.625	GeV
Photon Energy	E_{ph}	13.800	15.759	13.800	15.759	keV
Rigidity	$B\rho$	42.5	45.4	42.5	45.4	Tm
Integrated Magnetic Dipole Field	$(BL)_{dipole}$	0.178	0.190	0.190	0.190	Tm
Dipole Bending Angle	Θ_{bend}	4.181	4.181	4.460	4.181	mrad
Dipole Bending Radius	ρ_{dipole}	85.1	85.1	79.7	85.1	m
Electron Beam Displacement	$\Delta x_{chicane}$	4.000	4.000	3.814	3.575	mm
Phase Integral	PI	0.05300	0.06052	0.05300	0.05318	T^2m^3
Extra Path Length	Δs_c	14.7	14.7	14.7	12.9	μm
Time Delay	Δt_c	48.9	48.9	48.9	42.9	fs
Bunch Lengthining	R_{56}	29.30	29.30	29.30	25.75	μm

4. SUMMARY

The LCLS-II-HE project is proposing to upgrade the current HXRSS chicane girder. The proposed modifications that are relevant for the considerations of this document, are the increase in separation between the two center chicane dipole magnets by 0.20362 m. The proposed modifications have only minor impact on beam performance. The impact can be mitigated by increasing the strengths of each of the four chicane dipoles by 6.68% up to an electron energy of 12.75 GeV (photon energy of 13.8 keV). Between that energy and 13.625 GeV (15.759 keV) the maximum chicane delay is reduced down to 42.9 fs, which is still above the desired maximum delay of 40 fs. Also, all the energies at which limitations occur are above 12 keV, the highest energy for which HXRSS based on the diamond crystal is supposed to work. The bottom line is that this part of the proposed upgrade is not a concern.

References

[1] Y. Feng, "Hard X-ray Self-Seeding (HXRSS) System Requirements Document," 23 February 2017. LCLSII-3.2-PR-0102-R1.